

# Asymmetric Anion- $\pi$ Catalysis of Iminium/Nitroaldol Cascades To Form Cyclohexane Rings with Five Stereogenic Centers Directly on $\pi$ -Acidic Surfaces

Le Liu,<sup>†</sup> Yoann Cotelte,<sup>†</sup> Alyssa-Jennifer Avestro,<sup>†,‡,§</sup> Naomi Sakai,<sup>†</sup> and Stefan Matile<sup>\*,†</sup>

<sup>†</sup>Department of Organic Chemistry, University of Geneva, Geneva, Switzerland

<sup>‡</sup>Department of Chemistry, Northwestern University, Evanston, Illinois 60208, United States

**S** Supporting Information

**ABSTRACT:** Anion- $\pi$  interactions have been introduced to catalysis only recently, and evidence for their significance is so far limited to one classical model reaction in enolate and enamine chemistry. In this report, asymmetric anion- $\pi$  catalysis is achieved for the first time for a more demanding cascade process. The selected example affords six-membered carbocycles with five stereogenic centers in a single step from achiral and acyclic substrates. Rates, yields, turnover, diastereo- and enantioselectivity are comparable with conventional catalysts. Rates and stereoselectivity increase with the  $\pi$ -acidity of the new anion- $\pi$  catalysts. Further support for operational anion- $\pi$  interactions in catalysis is obtained from inhibition with nitrate. As part of the stereogenic cascade reaction, iminium chemistry and conjugate additions are added to the emerging repertoire of asymmetric anion- $\pi$  catalysis.

The integration of unorthodox noncovalent interactions into functional systems is of fundamental importance.<sup>1</sup> Current interest focuses on anion- $\pi$  interactions<sup>1-4</sup> and  $\sigma$ -hole interactions<sup>2</sup> such as halogen bonds,<sup>5</sup> the underrecognized counterparts of cation- $\pi$  interactions<sup>6</sup> and hydrogen bonds, respectively. With regard to catalysis, halogen bonds receive much attention,<sup>1,7</sup> whereas the formal introduction of anion- $\pi$  interactions has been only as recent as 2013.<sup>8</sup> Explicitly realized examples, with evidence for increasing activity with increasing  $\pi$ -acidity, reach from the initial Kemp elimination<sup>8</sup> to more relevant model reactions for enolate<sup>9</sup> and asymmetric enamine chemistry.<sup>10</sup> Contributions from anion- $\pi$  interactions have also been suggested to operate in catalysts for asymmetric Henry reactions<sup>11</sup> and anion-binding catalysis.<sup>12</sup> The general idea with anion- $\pi$  catalysis is to stabilize anionic reactive intermediates and transition states on the  $\pi$ -acidic surface of electron-deficient aromatic systems with positive quadrupole moments.<sup>8-10</sup> This concept is complementary to the conventional stabilization of cationic intermediates on  $\pi$ -basic surfaces, known from biosynthesis and increasingly implemented in organocatalysis.<sup>1,6</sup> In this report, the scope of anion- $\pi$  catalysis is expanded to more demanding cascade processes that include also reactions that are new to the topic (iminium chemistry, etc.), stereoselectivities beyond the limits of conventional catalysts, and selective anion- $\pi$  inhibition.

The reaction between enal **1** and dinitropropane **2** was selected because it affords cyclohexane rings **3** with five consecutive stereocenters in a cascade that covers iminium chemistry, conjugate additions, and Henry reactions (Figure 1a).<sup>13</sup> To catalyze this process on  $\pi$ -acidic surfaces, trifunctional systems **4-9** and bifunctional controls **10** and **11** were designed and synthesized (Figure 1b). They all contain a *trans*-cyclohexyldiamine as a rigidified Leonard turn<sup>14</sup> that places a tertiary amine<sup>13</sup> next to the  $\pi$ -acidic surface of a naphthalenediimide<sup>15</sup> (NDI). These turns have been intro-

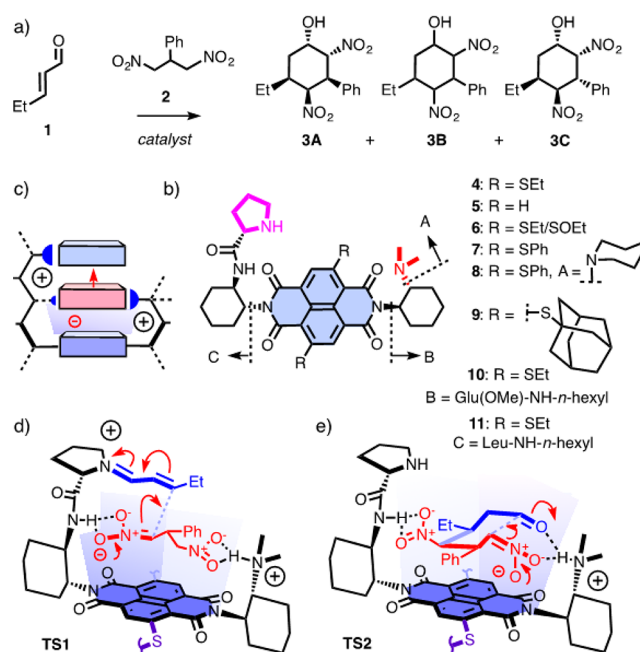


**Figure 1.** (a) Cascade reaction catalyzed by (b) anion- $\pi$  systems **4-11**, with notional transition states **TS1** (in schematic side view (c) and full structure (d)) and **TS2** (e). Blue areas highlight  $\pi$ -acidic surfaces and possible contributions of anion- $\pi$  interactions to TS stabilization (and iminium cations, c). Compound **6** is a mixture of sulfoxide stereoisomers concerning the position of R. In **9**, (*S,S*)-instead of (*R,R*)-cyclohexyldiamine was used to attach the proline (the stereochemistry of *trans*-cyclohexyldiamine did not influence the catalytic activity significantly<sup>19</sup>).

Received: May 13, 2016

Published: June 21, 2016

duced as powerful tools to run reactions on aromatic surfaces and enable also weak aromatic interactions to contribute to catalysis.<sup>14</sup>

Contrary to enamine chemistry,<sup>16</sup> cationic iminium chemistry<sup>13,17</sup> should be destabilized rather than stabilized on  $\pi$ -acidic surfaces. In 4–10, a proline is positioned quite far from the  $\pi$ -acidic surface to avoid such cation– $\pi$  repulsion. Within this electron-deficient “LUMO space,” substrate 2 should become deprotonated, producing a  $\pi$ -acid-stabilized nitronate intermediate that is ready to undergo a conjugate addition to the iminium cation (Figure 1d). The resulting electron acceptor–donor–acceptor triad in transition state 1 (TS1) is a possibly general motif obtained by intriguing “LUMO tweezers” (Figure 1c). Conjugate addition is followed by the hydrolysis of the enamine and the formation of another  $\pi$ -stabilized nitronate anion before the intramolecular Henry reaction<sup>11,18</sup> outlined in TS2 takes place (Figure 1e). This cyclization, perhaps stabilized by oxyanion– $\pi$  interactions and possible hydrogen bonding to the amide hydrogen, affords product 3.

Catalysts 4–11 were accessible in a few steps from commercially available starting materials. Details of their syntheses can be found in the Supporting Information (SI).<sup>19</sup> The initial evaluation was performed with catalyst 7. This catalyst carries two phenylsulfide substituents in the NDI core to increase  $\pi$ -acidity relative to ethylsulfides<sup>20</sup> and maximize stereoselectivity by peripheral crowding at the edge of the central  $\pi$ -surface.<sup>21</sup>

In the presence of 7, the reaction between enal 1 and dinitropropane 2 afforded cyclohexane 3 in good yield and stereoselectivity in all solvents except the more polar mixtures of CDCl<sub>3</sub> and CD<sub>3</sub>OD (Table 1, entries 1–9). Aromatic solvents were particularly interesting because of eventual interactions with the  $\pi$ -acidic surface in catalyst 7 and the

reactive intermediates.<sup>21,22</sup> Performances in benzene were indeed slightly better than in toluene (Table 1, entry 5 vs 6). Clearly lower enantioselectivity obtained in the  $\pi$ -basic 1,3-DMB compared to benzene indicated that the eventual formation of aromatic donor–acceptor complexes<sup>23</sup> with the central  $\pi$ -surface hinders rather than helps asymmetric anion– $\pi$  catalysis (Table 1, entry 7). Although still slightly  $\pi$ -basic,  $\pi$ – $\pi$  stacking with complementary, electron-deficient nitrobenzene could further increase the electron deficiency of the central  $\pi$ -surface and thus enhance anion– $\pi$  catalysis. The highest yield, diastereoselectivity, and enantioselectivity obtained with catalyst 7 in nitrobenzene were in agreement with these expectations (Table 1, entry 9). Because of poor solubility of the catalysts, the  $\pi$ -acidic hexafluorobenzene<sup>22</sup> could only be tested with chloroform as a cosolvent. Nevertheless, the obtained results, comparable to those in nitrobenzene, could be considered as further support of the above-mentioned hypothesis (Table 1, entry 8).

Substitution of the phenyl sulfides in the NDI core of catalyst 7 by ethyl sulfides in catalyst 4 clearly reduced activity in nitrobenzene, particularly with regard to enantioselectivity ( $\Delta ee = -18\%$ , Figure 1, Table 1, entry 9 vs 10). The same trends were observed in other solvents. These changes suggested that peripheral crowding at the edge of the  $\pi$ -surface contributes to stereoselectivity of the anion– $\pi$  catalyst. The slight increase in  $\pi$ -acidity by  $-40$  meV of LUMO energy level<sup>20</sup> from ethyl sulfides in 4 to phenyl sulfides in 7 was too small to account for  $\Delta ee = +18\%$ . More significant increases in  $\pi$ -acidity in catalyst 5 without core substituents ( $-90$  meV vs 4)<sup>20</sup> and catalyst 6 with one ethyl sulfide and one ethyl sulfoxide in the core ( $-170$  meV vs 4)<sup>20</sup> caused less significant increases in enantioselectivity ( $\Delta ee = +3\%$ ,  $+13\%$ , Table 1, entries 13, 14 vs 10, Figures 1, 2b). With increasing  $\pi$ -acidity in this series 4–6, the rate of the reaction increased as well. An almost linear correlation was found between the half-life of the substrate and the LUMO energy of the NDI in catalysts 4–6 (Figure 2a). The coincidence of increasing  $\pi$ -acidity, rate (Figure 2a), and enantioselectivity (Figure 2b) provided compelling<sup>1,6,8–10,14</sup>

Table 1. Screening of Catalysts and Solvents<sup>a</sup>

cat. <sup>b</sup>	solvents <sup>c</sup>	$\eta$ (%) <sup>d</sup>	dr <sup>e</sup>	ee (%) <sup>f</sup>	
1	7	CD <sub>2</sub> Cl <sub>2</sub>	80	61:21:18	50
2	7	CD <sub>3</sub> CN	72	50:20:30	39
3	7	CDCl <sub>3</sub> /CD <sub>3</sub> OD 1:1	0	–	–
4	7	CDCl <sub>3</sub>	78	57:27:16	50
5	7	Toluene	60	59:18:23	47
6	7	Benzene	74	59:15:26	50
7	7	1,3-DMB	81	61:18:21	37
8	7	C <sub>6</sub> F <sub>6</sub> /CDCl <sub>3</sub> 1:1	86	62:25:13	48
9	7	Nitrobenzene	90	63:19:18	58
10	4	Nitrobenzene	84	56:20:24	40
11	4	C <sub>6</sub> F <sub>6</sub> /CDCl <sub>3</sub> 1:1	84	56:20:24	48
12	4	Benzene	82	53:25:22	30
13	5	Nitrobenzene	87	61:18:21	43
14	6 <sup>g</sup>	Nitrobenzene	83	56:15:29	53
15	8	Nitrobenzene	88	69:12:19	67
16	9	Nitrobenzene	91	65:14:21	70
17	10	Nitrobenzene	0	–	–
18	12 + 13	Nitrobenzene	81	60:21:19	-46

<sup>a</sup>With 1.0 M 1, 0.5 M 2, 20 mol % catalyst. <sup>b</sup>Catalysts (Figures 1, 2).

<sup>c</sup>Solvents: DMB = Dimethoxybenzene. <sup>d</sup>Total yield of 3 determined by NMR after consumption of 2 (48–60 h (4–10), 96 h (12 + 13)).

<sup>e</sup>Diastereomeric ratio of three major isomers 3A/3B/3C (Figure 1).

<sup>f</sup>Enantiomeric excess for 3A; negative ee's indicate preference for the opposite enantiomer of 3A. <sup>g</sup>Mixture of sulfoxide stereo- and regioisomers concerning the position of R.

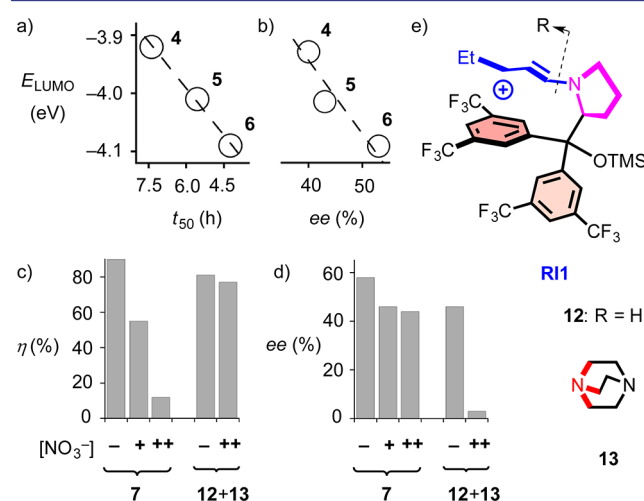


Figure 2. Dependence of (a) substrate half-life time ( $t_{50}$ ) and (b) ee on the  $\pi$ -acidity of catalysts 4–6 (indicated as LUMO energy of the NDIs<sup>20</sup>). (c) Total yield  $\eta$  after 48 h (7) or 96 h (12 + 13) and (d) ee of 3A obtained with 7 (left) and 12 + 13 (right) as a function of the concentration of Bu<sub>4</sub>NNO<sub>3</sub> (– = 0 M, + = 2.5 M, ++ = 5.0 M). (e) Structure of controls 12, 13 and intermediate R11.

corroboration that anion- $\pi$  interactions contribute to not only catalysis but also enantioselectivity, i.e. asymmetric catalysis.

Further improvements in catalyst design could be achieved by replacing the acyclic amine in **7** with a cyclic one in **8** (Figure 1). An  $ee = 67\%$  was the result, together with the highest diastereoselectivity observed for this reaction (Table 1, entry 15). Maximized peripheral crowding in three dimensions with adamantyl sulfides at the edge of the  $\pi$ -surface in **9** gave  $ee = 70\%$ , the best enantioselectivity of the series (Table 1, entry 16). These trends are particularly important because they provide clear guidelines toward further improving asymmetric anion- $\pi$  catalysis.

The bifunctional catalyst **10** without tertiary amine was inactive (Table 1, entry 17). This control was also important to confirm that the cascade reaction occurs between the proline and the tertiary amine in the trifunctional catalysts **4**–**9**, that is on the  $\pi$ -acidic surface.

The original mix of Jørgensen–Hayashi catalyst **12** and DABCO (**13**) as an additional amine base has been reported to give, at best, 90%  $ee$  and  $dr = 57:29:14$  in  $\text{CH}_2\text{Cl}_2$ .<sup>13</sup> However, under conditions optimized for anion- $\pi$  catalyst **7**, this noncovalent system **12** + **13** did not perform equally well (Figure 2e, Table 1, entry 18). In nitrobenzene, the best  $ee = 70\%$  obtained with anion- $\pi$  catalysts, i.e., the overcrowded adamantylsulfides **9**, was  $\Delta ee = +24\%$  better than the conventional system **12** + **13** with  $ee = -46\%$  (Table 1, entry 16 vs 18). Interestingly, the absolute configuration of the main diastereomer **3A** obtained with anion- $\pi$  catalysts **4**–**9** and Jørgensen's system **12** + **13** was opposite. Thus, with anion- $\pi$  catalysts the stereodetermining nitronate addition occurs from the more hindered side of the proline fragment due to the stabilization of the nitronate by the  $\pi$ -acidic surface (Figure 1d). In the conventional system **12**, this more hindered side of the pyrrolidine ring is shielded in intermediate **RII**, and the conjugate addition occurs from the less hindered side of the heterocycle (Figure 2e). The diastereoselectivity of anion- $\pi$  catalysts, best with  $dr = 69:12:19$  for **8**, is clearly beyond the values reported for the conventional system **12** + **13** (Table 1, entry 15 vs 18).

As confirmed for the MacMillan catalyst,<sup>24</sup> it is conceivable that the conventional catalyst **12** stabilizes the Leonard-turned<sup>14</sup> iminium intermediate with cation- $\pi$  interactions (**RII**, Figure 2e). Noncovalent hybrid systems with additional  $\pi$ -acidic surfaces, either **12** + **11** or **10** + **13**, did not improve performance (Table 2, entries 8, 9). The change from 20 to 5 mol % catalyst did not affect the results with the covalent anion- $\pi$  catalyst **7** (89%,  $ee = 58\%$ , Table 2, entry 2). With the conventional catalyst **12** + **13**, the same lowering in catalyst loading reduced yield and enantioselectivity (74%,  $ee = -39\%$  (Table 2, entry 6).

In the presence of nitrate, the yield obtained with catalyst **7** decreased with  $\text{IC}_{50} \approx 2.5$  M and reach almost full inhibition with 5.0 M  $\text{Bu}_4\text{NNO}_3$  (Figure 2c; Table 2, entry 3). The  $ee$  of product **3A** was not strongly affected by nitrate inhibition (Figure 2d; Table 2, entry 3). In contrast, the yield dropped only to 46% with 5.0 M  $\text{Bu}_4\text{NPF}_6$  (Table 2, entry 4). These findings were consistent with the selective inhibition of catalyst **7** by nitrate- $\pi$  interactions,<sup>25</sup> that is the existence and functional significance of asymmetric anion- $\pi$  catalysis. This important conclusion was supported by the inability of 5.0 M  $\text{Bu}_4\text{NNO}_3$  to inhibit the original noncovalent system **12** + **13** (Figure 2c; Table 2, entry 7). However, the enantioselectivity of the original mixture **12** + **13** completely vanished in the

Table 2. Catalyst Inhibition and Comparative Evaluation<sup>a</sup>

	cat. <sup>b</sup>	mol % <sup>c</sup>	additive <sup>d</sup>	$\eta$ (%) <sup>e</sup>	$dr$ <sup>f</sup>	$ee$ (%) <sup>g</sup>
1	7	20		90	63:19:18	58
2	7	5		89	63:13:24	58
3	7	20	$\text{NO}_3^-$	10	53:23:24	44
4	7	20	$\text{PF}_6^-$	46	nd	nd
5	<b>12</b> + <b>13</b>	20		81	60:21:19	-46
6	<b>12</b> + <b>13</b>	5		74	58:24:18	-39
7	<b>12</b> + <b>13</b>	20	$\text{NO}_3^-$	77	62:16:22	-3
8	<b>12</b> + <b>11</b>	20		79	48:25:27	-54
9	<b>10</b> + <b>13</b>	20		80	53:24:23	38

<sup>a</sup>Standard conditions: 1.0 M **1**, 0.5 M **2**, catalyst, nitrobenzene, 20 °C.

<sup>b</sup>Catalysts (Figures 1, 2). <sup>c</sup>Mol % of pyrrolidine containing catalyst (**7**, **12**, and **10**). Noncovalent amines were used equimolar. <sup>d</sup>Additives.  $\text{NO}_3^-$ : 5.0 M  $\text{Bu}_4\text{NNO}_3$ .  $\text{PF}_6^-$ : 5.0 M  $\text{Bu}_4\text{NPF}_6$ . <sup>e</sup>Total yield of **3** determined by NMR after consumption of **2** (48–60 h (**7**, **10** + **13**), 80 h (**12** + **11**), 96 h (**12** + **13**)). <sup>f</sup>Diastereomeric ratio of three major isomers **3A**:**3B**:**3C** (Figure 1). <sup>g</sup>Enantiomeric excess for **3A**; negative  $ee$ 's indicate opposite enantiomer.

presence of nitrate (Figure 2d; Table 2, entry 7). This finding suggested that ion pairing with the iminium cation governs the enantioselectivity of the noncovalent original **12** + **13** and confirmed that anion- $\pi$  catalyst **7** operates differently.

In summary, anion- $\pi$  catalysts are introduced for cascade processes that afford cyclohexane rings with five stereocenters in one step. The observed dependence of rate and selectivity on  $\pi$ -acidity, and inhibition with nitrate provide experimental support for the contribution of anion- $\pi$  interactions to the stereoselective stabilization of the anionic transition states. Under conditions optimized in their favor, anion- $\pi$  catalysts operate with yields, rates, and enantioselectivities that exceed those of conventional catalysts, and the diastereoselectivity reaches a new absolute maximum.

## ■ ASSOCIATED CONTENT

### 📄 Supporting Information

The Supporting Information is available free of charge on the ACS Publications website at DOI: 10.1021/jacs.6b04936.

Detailed experimental procedures (PDF)

## ■ AUTHOR INFORMATION

### Corresponding Author

\*stefan.matile@unige.ch

### Present Address

<sup>§</sup>Department of Chemistry, Durham University, Durham, United Kingdom.

### Notes

The authors declare no competing financial interest.

## ■ ACKNOWLEDGMENTS

We thank the NMR and the Sciences Mass Spectrometry (SMS) platforms for services, and the University of Geneva, the European Research Council (ERC Advanced Investigator), the Swiss National Centre of Competence in Research (NCCR) Chemical Biology, the NCCR Molecular Systems Engineering, and the Swiss NSF for financial support. A.-J.A. thanks the US NSF for a GROW Fellowship and the Swiss SERI/FCS for a Government Excellence Scholarship.

## REFERENCES

- (1) Zhao, Y.; Cotellet, Y.; Sakai, N.; Matile, S. *J. Am. Chem. Soc.* **2016**, *138*, 4270–4277.
- (2) Bauzá, A.; Mooibroek, T. J.; Frontera, A. *ChemPhysChem* **2015**, *16*, 2496–2517.
- (3) (a) Giese, M.; Albrecht, M.; Rissanen, K. *Chem. Commun.* **2016**, *52*, 1778–1795. (b) Chifotides, H. T.; Dunbar, K. R. *Acc. Chem. Res.* **2013**, *46*, 894–906. (c) Frontera, A.; Gamez, P.; Mascal, M.; Mooibroek, T. J.; Reedijk, J. *Angew. Chem., Int. Ed.* **2011**, *50*, 9564–9583.
- (4) See refs 1 and 10 for comments on the term “anion- $\pi$  interactions.”
- (5) Cavallo, G.; Metrangolo, P.; Milani, R.; Pilati, T.; Priimagi, A.; Resnati, G.; Terraneo, G. *Chem. Rev.* **2016**, *116*, 2478–2601.
- (6) (a) Knowles, R. R.; Lin, S.; Jacobsen, E. N. *J. Am. Chem. Soc.* **2010**, *132*, 5030–5032. (b) Zhang, Q.; Tiefenbacher, K. *J. Am. Chem. Soc.* **2013**, *135*, 16213–16219.
- (7) (a) Jungbauer, S. H.; Huber, S. M. *J. Am. Chem. Soc.* **2015**, *137*, 12110–12120. (b) Zong, L.; Ban, X.; Kee, C. W.; Tan, C.-H. *Angew. Chem., Int. Ed.* **2014**, *53*, 11849–11853.
- (8) Zhao, Y.; Domoto, Y.; Orentas, E.; Beuchat, C.; Emery, D.; Mareda, J.; Sakai, N.; Matile, S. *Angew. Chem., Int. Ed.* **2013**, *52*, 9940–9943.
- (9) (a) Zhao, Y.; Benz, S.; Sakai, N.; Matile, S. *Chem. Sci.* **2015**, *6*, 6219–6223. (b) Miros, F. N.; Zhao, Y.; Sargsyan, G.; Pupier, M.; Besnard, C.; Beuchat, C.; Mareda, J.; Sakai, N.; Matile, S. *Chem. - Eur. J.* **2016**, *22*, 2648–2657.
- (10) Zhao, Y.; Cotellet, Y.; Avestro, A.-J.; Sakai, N.; Matile, S. *J. Am. Chem. Soc.* **2015**, *137*, 11582–11585.
- (11) Alegre-Requena, J. V.; Marqués-López, E.; Herrera, R. P. *Adv. Synth. Catal.* **2016**, *358*, 1801–1809.
- (12) Berkessel, A.; Das, S.; Pekel, D.; Neudörfl, J.-M. *Angew. Chem., Int. Ed.* **2014**, *53*, 11660–11664.
- (13) (a) Reyes, E.; Jiang, H.; Milelli, A.; Elsner, P.; Hazell, R. G.; Jørgensen, K. A. *Angew. Chem., Int. Ed.* **2007**, *46*, 9202–9205. (b) Jensen, K. L.; Dickmeiss, G.; Jiang, H.; Albrecht, L.; Jørgensen, K. A. *Acc. Chem. Res.* **2012**, *45*, 248–264.
- (14) Cotellet, Y.; Benz, S.; Avestro, A.-J.; Ward, T. R.; Sakai, N.; Matile, S. *Angew. Chem., Int. Ed.* **2016**, *55*, 4275–4279.
- (15) Suraru, S. L.; Würthner, F. *Angew. Chem., Int. Ed.* **2014**, *53*, 7428–7448.
- (16) (a) Hayashi, Y.; Samanta, S.; Gotoh, H.; Ishikawa, H. *Angew. Chem., Int. Ed.* **2008**, *47*, 6634–6637. (b) Mukherjee, S.; Yang, J. W.; Hoffmann, S.; List, B. *Chem. Rev.* **2007**, *107*, 5471–5569.
- (17) Volla, C. M. R.; Atodiresei, I.; Rueping, M. *Chem. Rev.* **2014**, *114*, 2390–2431.
- (18) Blümel, M.; Chauhan, P.; Hahn, R.; Raabe, G.; Enders, D. *Org. Lett.* **2014**, *16*, 6012–6015.
- (19) See SI.
- (20) Miros, F. N.; Matile, S. *ChemistryOpen*, in press (DOI: [10.1055/s-0035-1561383](https://doi.org/10.1055/s-0035-1561383)).
- (21) Akamatsu, M.; Matile, S. *Synlett* **2016**, *27*, 1041–2046.
- (22) Lattanzi, A.; De Fusco, C.; Russo, A.; Poater, A.; Cavallo, L. *Chem. Commun.* **2012**, *48*, 1650–1652.
- (23) (a) Ponnuswamy, N.; Pantos, G. D.; Smulders, M. M. J.; Sanders, J. M. K. *J. Am. Chem. Soc.* **2012**, *134*, 566–573. (b) Gabriel, G. J.; Iverson, B. L. *J. Am. Chem. Soc.* **2002**, *124*, 15174–15175.
- (24) Holland, M. C.; Paul, S.; Schweizer, W. B.; Bergander, K.; Mück-Lichtenfeld, C.; Lakhdar, S.; Mayr, H.; Gilmour, R. *Angew. Chem., Int. Ed.* **2013**, *52*, 7967–7971.
- (25) (a) Giese, M.; Albrecht, M.; Ivanova, G.; Valkonen, A.; Rissanen, K. *Supramol. Chem.* **2012**, *24*, 48–55. (b) Wang, D.-X.; Wang, M.-X. *J. Am. Chem. Soc.* **2013**, *135*, 892–897. (c) Adriaenssens, L.; Estarellas, C.; Vargas Jentzsch, A.; Martínez Belmonte, M.; Matile, S.; Ballester, P. *J. Am. Chem. Soc.* **2013**, *135*, 8324–8330.